объединенный
институт
ядерных
исследований
дубна

E1-87-265

PRODUCTION OF $\overline{D}^{\circ}$ AND D^{-} MESONS IN NEUTRON-CARBON INTERACTIONS AT 40-70 GeV

BIS-2 Collaboration: Berlin - Budapest - Dubna - Moscow - Prague - Sofia - Tbilisi

Submitted to "Zeitschrift für Physik C"

1987

A.N.Aleev, V.A.Arefiev, V.P.Balandin, V.K.Berdyshev, V.K.Birulev, A.S.Chvyrov, I.I.Evsikov, T.S.Grigalashvili, B.N.Gus'kov, K.Hiller, I.M.Ivanchenko, I.N.Kakurin, M.N.Kapishin, N.N.Karpenko, D.A.Kirillov, I.G.Kosarev, V.R.Krastev, N.A.Kus'min, M.F.Likhachev, A.L.Lyubimov, A.N.Maksimov, P.V.Moisenz, A.N.Morozov, V.V.Pal'chik, A.V.Pose, A.Prokes, V.E.Simonov, L.A.Slepets, M.Smizanska, G.G.Takhtamyshev, P.T.Todorov, N.V.Vlasov, A.I.Zinchenko
Joint Institute for Nuclear Research, Dubna

I.Veres
Central Institute for Physics of the Hungarian Academy of Sciences, Budapest, Hungary

J.Klabuhn, H.Nowak, S.Nowak, H.-E.Ryseck
Institute of High Energy Physics of the GDR Academy of Sciences, Berlin-Zeuthen, GDR

A.S.Belousov, E.G.Devitsin, A.M.Fomenko, V.A.Kozlov, E.I.Malinovsky, V.V.Pavlovskaya, S.Yu.Potashov, S.V.Rusakov, P.A.Smirnov, Yu.V.Soloviev, L.N.Shtarkov, A.R.Terkulov, Ya.A.Vazdik, M.V.Zavertyaev
Lebedev Physical Institute of the USSR Academy of Sciences, Moscow, USSR

T.B.Progulova, E.A.Chudakov
Institute of Nuclear Physics, Moscow State University, Moscow, USSR

J.Hladky, M.Novak, M.Vecko
Institute of Physics of the Czechoslovak Academy of Sciences, Prague, Czechoslovakia

V.D.Cholakov
Hilendarsky University of Plovdiv, Plovdiv, Bulgaria

V.D.Zayachky
Higher Chemical-Technological Institute, Sofia, Bulgaria

D.T.Burilkov, P.K.Markov, G.G.Sultanov, R.K.Trayanov
Institute of Nuclear Research and Nuclear Energetics of the Bulgarian Academy of Science, Sofia, Bulgaria

N.S.Amaglobeli, V.P.Dzhordzhadze, V.K.Kekelidze, N.L.Lomidze, G.I.Nikobadze, G.T.Tatishvili, R.G.Shanidze
Institute of High Energy Physics, Tbilisi State University, Tbilisi, USSR

1. INTRODUCTION

In the last few years hadronic charm production has been studied in a number of experiments over an energy range well above the charm threshold, either at the CERN ISR /1-4/ or at the FNAL and CERN high-energy proton accelerators /5-12/. At lower energies only Λ_c^+ production has been measured at the Serpukhov accelerator /13/. The production of $D/\bar{D}$ mesons at such low energies has not been observed up to now. From the comparison of Λ_c^+ and $D/\bar{D}$ cross sections the fractions of $\Lambda_c^+\bar{D}$ and $D\bar{D}$ final states can be estimated. Furthermore, data near the kinematical threshold are of interest in order to get more insight into the energy dependence of charm cross sections.

In this letter we present the first measurement of $\bar{D}^0$ and D^- production in neutron-carbon interactions at 40 - 70 GeV/c. The experiment was performed with the BIS-2 spectrometer at the Serpukhov accelerator. Recently our collaboration has published the results on Λ_c^+ production /13/. Continuing the analysis of the same data sample, we have found signals of $\bar{D}^0$ and D^- mesons in the decay modes $\bar{D}^0 \to K^+(892)\pi^-$ and $D^- \to K^+(892)\pi^-\pi^-$ /14/. The observed $\bar{D}$ mesons cover the kinematical region $x > 0.5$ and $p_T < 1$ GeV/c, where $x = 2p_L^*/\sqrt{s}$ is the fractional longitudinal momentum in the centre of mass system and p_T is the transverse momentum.

The main components of the BIS-2 spectrometer are a momentum analyzing magnet and 22 planes of multiwire proportional chambers (MWPCs) arranged upstream and downstream from the magnet. The magnet has an aperture of 100 * 30 cm^2 and an integral field of 2.1 T·m. The trigger was designed to select multiparticle events, which are typical for decays of charmed particles. Four or more charged particles were required to pass through the spectrometer. The spectrum of the neutron beam peaks near 40 GeV/c with a tail up to 70 GeV/c. For three different spectrometer configurations (target positions and length, positions of MWPCs and magnetic field polarity) 11.4*10^6 events were recorded corresponding to an integral luminosity of 1.9*10^{35} cm^{-2}. A more detailed description of the BIS-2 spectrometer is given elsewhere /15/.

In section 2 we describe the search for charm signals in the invariant mass spectra. The characteristics of $\bar{D}^0$ and D^- production are presented in section 3. In section 4, these characteristics are compared with the Λ_c^+ results from the same experiment and data from other experiments. Conclusions on the charm production mechanism in the very forward region are drawn. Section 5 is the summary.

2. INVARIANT MASS SPECTRA

Short-lived particles can be detected as signals in the invariant mass spectra of their decay particles. A good knowledge of the mass resolution and the mass scale is essential in this type of analysis. We have checked mass scale and resolution using the decays of strange particles, such as $\Lambda, \Sigma^{\pm}(1385), \Xi^-$ and $\Xi^0(1530)$ /16/. The identification of charged particles was not available, and mass values are simply assigned. The K_s^0 was detected as a pronounced peak in the $\pi^+\pi^-$ mass spectrum. The width of the signal is 8 MeV/c^2 at half maximum. For the further analysis 119000 events with K_s^0 candidates in the mass interval from 489 to 505 MeV/c^2 were selected. This mass slice includes 32 % background combinations.

First, the production of $D/\bar{D}$ mesons was searched for in the decay modes $D^{\pm} \to \bar{K}^0/K^0\pi^{\pm}$. The mass spectra of $K_s^0\pi^{\pm}$ combinations are shown in fig.1. They exhibit signals of the resonances $K^{\pm}(892)$.

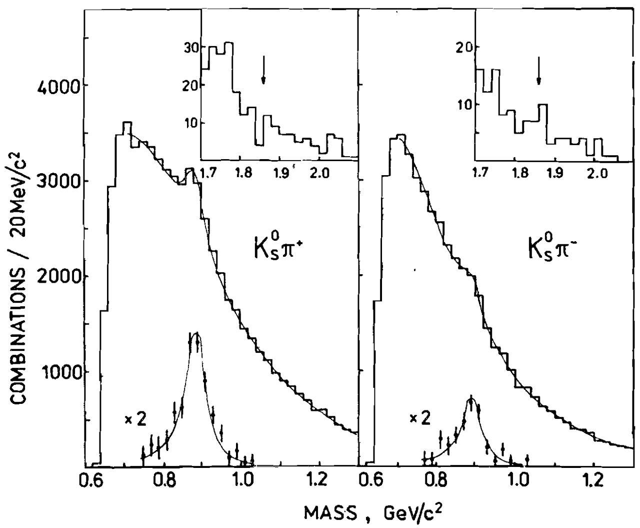

Fig.1. Invariant mass spectra of $K_s^0\pi^{\pm}$ combinations. The background-subtracted signals of $K^{\pm}(892)$ are also shown. The inserts show the $D^{\pm}$ mass regions and the arrows indicate the tabulated $D^{\pm}$ masses.

Fitting them by a Breit-Wigner function above an exponential background results in signals of 4000 $K^+(892)$ and 2200 $K^-(892)$. The $D^{\pm}$ mass regions are displayed in the inserts of fig.1. No indication of $D^{\pm}$ signals can be found.

Next, we looked for the decays $D^0/\bar{D}^0 \to \bar{K}^0/K^0\pi^+\pi^-$ and $D^{\pm} \to \bar{K}^0/K^0\pi^+\pi^-\pi^{\pm}$. The mass spectra of these decays are depicted in fig.2. They do not show any structure in the $D/\bar{D}$ mass regions. The upper limits of signals, which are equivalent to a 2 standard deviation effect in the mass interval from 1820 to 1900 MeV/c^2, are $N_{D^0/\bar{D}^0} = 44$, $N_{D^-} = 39$ and $N_{D^+} = 42$ combinations.

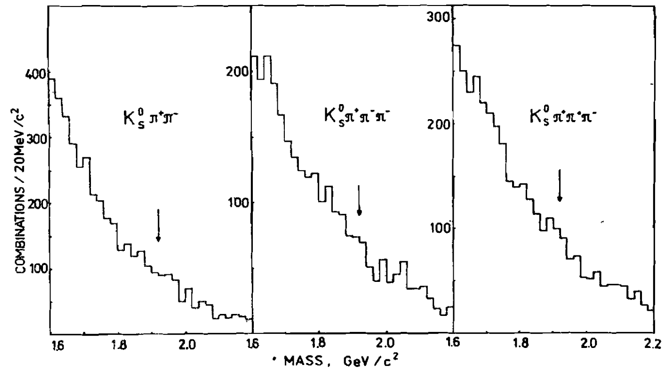

Fig.2. Invariant mass spectra of $K_s^0\pi^+\pi^-$ and $K_s^0\pi^+\pi^-\pi^{\pm}$ combinations. The arrows show the expected location of the $D/\bar{D}$ signals.

An improvement in the charm signal-to-background ratio is achieved by the selection of its cascade decay via K(892). The subchannel with K(892) represents a large fraction of the $D/\bar{D}$ decays into $\bar{K}/K$ plus pions and the suppression of background is expected to be much stronger than the loss of signal /17/. Fig.3 shows the mass distributions of $K^+(892)\pi^-$ and $K^+(892)\pi^-\pi^-$ combinations. Small peaks are visible at the positions of $\bar{D}^0$ and D^- masses. An additional background suppression is achieved when the events with $K_s^0\pi^-$ masses close to $K^-(892)$ or $K_2^-(1430)$ are excluded. These conditions reduce also the contribution of the resonances $K_3^0(1780)$ and $K_3^{\pm}(1780)$ on the low mass side of the $\bar{D}^0/D^-$ peaks. The $K^-(892)$ and $K_2^-(1430)$ are defined by the mass slices from 840 to 940 MeV/c^2 and 1330 to 1530 MeV/c^2, respectively. The inserts of fig.3 show the peak regions under these additional conditions.

A fit to the mass spectra by an exponential background and a Gaussian yields the central mass values $M_{\bar{D}^0} = (1868 \pm 8)$ MeV/c^2 and

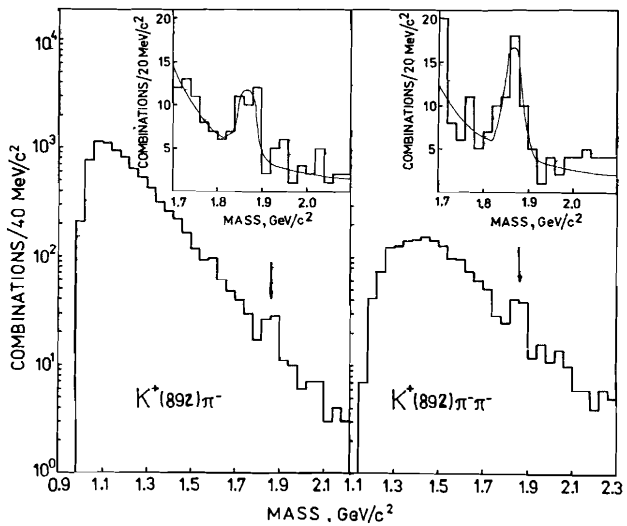

Fig.3. Invariant mass spectra of $K^{*}(892)\pi^{-}$ and $K^{*}(892)\pi^{-}\pi^{-}$ combinations. The inserts show the $\bar{D}^0/D^-$ mass regions where the events with $K^-(892)$ or $K_2^-(1430)$ candidates are excluded.

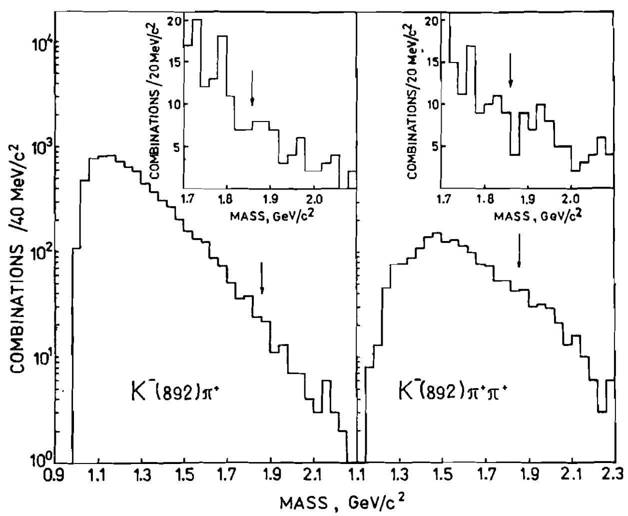

Fig.4. Invariant mass spectra of $K^-(892)\pi^+$ and $K^-(892)\pi^+\pi^+$ combinations. The inserts show the D^0/D^+ mass regions where the events with $K^{*}(892)$ or $K^{*}(1430)$ candidates are excluded. The arrows indicate the tabulated D^0/D^+ masses.

$M_{D^-} = (1869 \pm 8)$ MeV/c^2, which are in good agreement with the tabulated values /17/. The widths of the peaks, $\Gamma_{\bar{D}^0} = (37 \pm 14)$ MeV/c^2 and $\Gamma_{D^-} = (37 \pm 11)$ MeV/c^2, are compatible with the expected mass resolution. The mass values and the narrow widths of the peaks allow us to conclude that the signals arise from weak decays of the charmed mesons $\bar{D}^0$ and D^-. The same arguments exclude an interpretation of the signals as a known kaon resonance. The fit results in the signals of (21 ± 6) $\bar{D}^0$ and (32 ± 7) D^- corresponding to a statistical significance of 5 and 7 standard deviations, respectively. The combination-to-event ratio in the peak region is nearly one.

No statistically significant enhancements of the charge conjugated mesons D^0 and D^+ decaying into $K^-(892)$ are observed. The mass spectra of $K^-(892)\pi^+$ and $K^-(892)\pi^+\pi^+$ combinations are given in fig.4. The selection criteria are the same as for $K^+(892)\pi^-$ and $K^+(892)\pi^-\pi^-$ combinations. The inserts of fig.4 show the D mass regions in which events with $K_s^0\pi^+$ masses close to $K^+(892)$ or $K_2^+(1430)$ are excluded.

3. CROSS SECTIONS AND MOMENTUM SPECTRA

In this section we determine the $\bar{D}^0$ and D^- cross sections for neutron-carbon interactions in the kinematical region, where our spectrometer is sensitive: $x > 0.5$ and $p_T < 1$ GeV/c. The cross sections per nucleon for $x > 0$ are extrapolated in section 4.

The acceptance of the apparatus was calculated by Monte-Carlo technique. We have simulated the following types of reactions: the diffractive production of a $\Lambda_c^+\bar{D}$ system, the semi-inclusive production of $\bar{D}$ accompanied by Λ_c^+, and the semi-inclusive production of $\bar{D}$ accompanied by Λ_c^+, nucleons and pions. The resulting acceptance over a two-dimensional p_L-p_T plot is nearly model-independent. For different reactions the acceptances integrated over the sensitive kinematical region differ by less than 10 %. The useful beam momentum range due to the spectrometer acceptance and trigger conditions is 40 - 70 GeV/c.

The partial cross section is given by:

$$\sigma_{\bar{D}} \cdot BR = N_{\bar{D}} \,/\, (L * a_{\bar{D}}), \qquad (1)$$

where $N_{\bar{D}}$, L, $a_{\bar{D}}$ and BR are the number of $\bar{D}$ events, luminosity, acceptance including trigger conditions and branching ratio, respectively. Using formula (1), we get the following partial cross sections: $\sigma_{\bar{D}^0} \cdot BR_1 = (2.0 \pm 0.7)$ μb and $\sigma_{D^-} \cdot BR_2 = (3.9 \pm 1.3)$ μb per carbon nucleus. The quoted errors do not include the overall normalization error connected with the intensity of the neutron beam. To estimate this uncertainty, we have calculated the cross sections by an independent method. The cross section $\sigma_{K^0 + \geq 2}$ of the well-measured reaction with K^0_s plus two or more charged particles in the final state was used for normalization of the charm yields. Formula (1) is modified as follows:

$$\sigma_{\bar{D}} \cdot BR = (N_{\bar{D}}/N_{K^0_s + \geq 2}) * (a_{K^0_s + \geq 2}/a_{\bar{D}}) * \sigma_{K^0_s + \geq 2} * BR_{K^0_s} \quad (2)$$

The cross section $\sigma_{K^0_s + \geq 2}$ for neutron-carbon interactions was estimated using the differential and topological cross sections of pp reactions and the atomic weight dependence of pA reactions /18/. Formula (2) gives the values: $\sigma_{\bar{D}^0} \cdot BR_1 = (2.7 \pm 1.0)$ μb and $\sigma_{D^-} \cdot BR_2 = (5.3 \pm 1.8)$ μb per carbon nucleus. As can be seen, the results from both methods agree indicating that the overall normalization error is less than 50 %. In further extrapolations the partial cross sections resulting from formula (1) will be used.

To evaluate inclusive cross sections, the corrections for unseen decay modes have to be done. The branching ratios were measured for the decays $\bar{D}^0 \rightarrow K^0\pi^+\pi^-$ (8.5 $\pm$ 1.4) %, $\bar{D}^0 \rightarrow K^+(892)\pi^-$(7.1 $\pm$ 2.5)% and $D^- \rightarrow K^0\pi^+\pi^-\pi^-$ (15.2 $\pm$ 5.8) % /17/. The observed signals can be a mixture of nonresonant decays and resonant decays because the selection of $K^+(892)$ includes a large fraction of nonresonant $K^0_s\pi^+$ combinations (see fig.1). Therefore the branching ratios BR_1 and BR_2 have to be values between those for the resonant subchannels with $K^+(892)$ and the full channels $\bar{D}^0 \rightarrow K^0\pi^+\pi^-$, $D^- \rightarrow K^0\pi^+\pi^-\pi^-$. For $\bar{D}^0$ both values are very close; so, the value of the resonant subchannel is used for BR_1 and the inclusive cross section $\sigma_{\bar{D}^0} = (28 \pm 14)$ μb per carbon nucleus is obtained. The lower limit of BR_2 is unknown because the branching ratio of the subchannel $D^- \rightarrow K^+(892)\pi^-\pi^-$ has not been measured to date. Using the ratio of the full channel $D^- \rightarrow K^0\pi^+\pi^-\pi^-$ yields the cross section $\sigma_{D^-} = (26 \pm 13)$ μb per carbon nucleus. From this value we can derive the lower limit $\sigma_{D^-} > 9$ μb per carbon nucleus with a 90 % confidence level assuming that the branching ratio of the full channel is an upper limit of BR_2.

We have also determined the production of $\bar{D}^0$ and D^- in dependence on the longitudinal and transverse momentum in the laboratory system. The background contribution is subtracted by estimation of the signal for each momentum bin. The signals are small, and the typical statistical error in a momentum bin is about 50 %.

The invariant longitudinal momentum spectra, after background subtraction and acceptance correction, are displayed in fig.5. The fits of a power law $F(x) \propto (1 - x)^N$ to the invariant momentum spectra

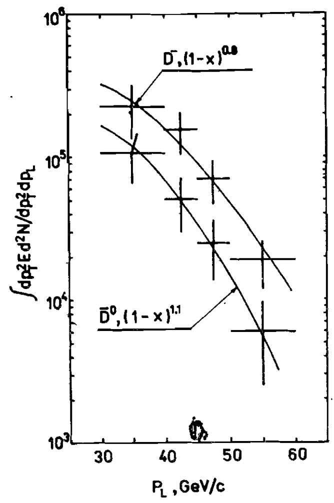

Fig.5 Invariant longitudinal momentum spectra of $\bar{D}^0$ and D^- mesons. The lines represent the fits of the power law dependence $(1 - x)^N$.

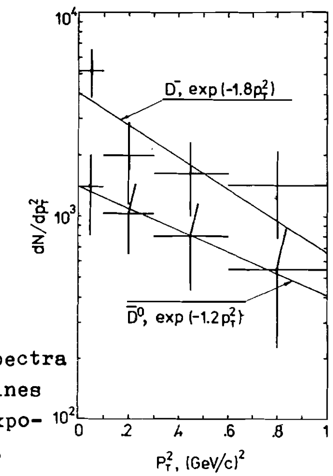

Fig.6 Transverse momentum spectra of $\bar{D}^0$ and D^- mesones. The lines represent the fits of the exponential function exp(-B p_T^2).

yield $N_{\bar{D}^0} = 1.1 \pm 0.5$(stat.) $\pm$ 0.4(syst.) and $N_{D^-} = 0.8 \pm 0.4 \pm 0.4$*). The systematic error reflects the uncertainty of the beam spectrum shape.

The background-subtracted and acceptance-corrected transverse momentum spectra are shown in fig.6. The spectra are compatible with an exponential decrease. Fitting the function exp(-B p_T^2) to the spectra, we obtain the slopes $B_{\bar{D}^0} = (1.2 ^{+1.1}_{-0.9})$ (GeV/c)$^{-2}$ and $B_{D^-} = (1.8 ^{+1.3}_{-1.0})$ (GeV/c)$^{-2}$. The average transverse momenta are (0.8 $\pm$ 0.3) GeV/c for $\bar{D}^0$ and (0.7 $\pm$ 0.2) GeV/c for D^- assuming the fitted p_T dependence in the full p_T region.

4. DISCUSSION OF THE RESULTS

The shape of the longitudinal momentum spectra is an essential feature of the underlying production mechanism. The spectra of $\bar{D}^0$ and D^- can be described in terms of $(1 - x)^N$ with $N \sim 1$. The quark counting rules predict the minimum value N = 3 for $\bar{D}$ production in a

*) The x value for an individual event cannot be calculated as a consequence of the unknown beam momentum for this event. So, the function F(x) has been transformed in the laboratory system using the known beam spectrum.

neutron beam [19]. This value is in disagreement with our data. Deviations from the counting rule predictions in the large x region were also observed in other reactions [20]. Hence, the counting rules often fail to describe spectra in the large x region, where most of our $\bar{D}$ mesons are populated. The disagreement between the counting rules and experimental spectra at large x can be due to contributions from resonance decays and/or diffractive processes, which raise the cross section at large x significantly. For Λ_c^+ production in the same experiment $N = 1.5 \pm 0.5$ was measured [13], which is in agreement with the counting rule prediction $N = 1$ [19]. As the comparison shows, the momentum spectra of Λ_c^+ and $\bar{D}$ in the beam fragmentation region are very similar. A natural explanation of this fact can be charm production in diffraction-like processes. The incoming neutron produces an excited state, which carries away most of the beam momentum and subsequently decays into $\bar{D}$ and Λ_c^+. In such a process similar spectra of $\bar{D}$ and Λ_c^+ in the forward region will be expected because their masses are not very different.

The inclusive $\bar{D}$ cross section in the region $x > 0.5$ is (54 ± 19) μb per carbon nucleus summarizing the $\bar{D}^0$ and D^- cross sections. For Λ_c^+ production we obtain in the same kinematical region a cross section of (80 ± 40) μb per carbon nucleus using the branching ratio $BR(\Lambda_c^+ \rightarrow \Lambda \pi^+\pi^+\pi^-) = 2.8$ % [21]. As can be seen, both cross sections have the same order of magnitude. This fact points to the dominance of $\Lambda_c^+\bar{D}$ over $D\bar{D}$ production in the large x region. The non-observation of the charge conjugated mesons D^0 and D^+ supports this hypothesis.

Now we estimate the cross sections per nucleon for $x > 0$. Because our experiment covers only the region $x > 0.5$, an assumption for the x dependence is required. The extrapolation is performed for two assumptions:

i) $\bar{D}$ mesons are produced associatively with Λ_c^+ baryons in diffraction-like processes according to the parametrization $d^2\sigma/dM^2dt \propto 1/M^2 \exp(-6t)$, where M is the mass of the $\Lambda_c^+\bar{D}$ system and t is the squared momentum transfer;

ii) the description $(1 - x)^N$ is valid for the whole x range using the values of N given by the experiment.

The atomic weight dependence of cross sections is generally described by a factor A^{α}, where A is the atomic weight number. For Λ_c^+ production we have measured $\alpha = 0.7 \pm 0.2$ using carbon, copper and aluminium as target materials [22]. This parametrization is assumed to be valid also for $\bar{D}$ production. The resulting cross sections

per nucleon in the region $x > 0$ for the extrapolations i) and ii) are given in table 1.

Tab.1. Inclusive $\bar{D}$ cross sections per nucleon $(x > 0)$. The x dependence for $x > 0$ is described by: i) diffractive $\Lambda_c^+\bar{D}$ production and ii) $(1 - x)^N$ behaviour. The cross sections are scaled by $A^{0.7}$.

REACTION	CROSS SECTION / μb	
	MODEL i)	MODEL ii)
$n + C \rightarrow \bar{D}^0 + X$	10 ± 5	32 ± 16
$n + C \rightarrow D^- + X$	9 ± 5	24 ± 12

Fig.7 presents a compilation of $D/\bar{D}$ cross sections $(x > 0)$ as a function of $\sqrt{s}$. The first measurements of D cross sections in pp interactions ($\sqrt{s} \sim 60$ GeV) were made in the ISR experiments [1-4]. These values were recalculated according to the new hadronic branching ratios [17]. At $\sqrt{s} \sim 26$ GeV, charm production in pp interactions was investigated in two LEBC-EHS experiments [5,6], and some measurements were made for pA interactions [7-11]. In order to get comparable values, the pA cross sections were divided by $A^{2/3}$ (see fig.7). With exception of the LEBC-EHS data [5,6], all cross sections depend strongly on the unknown production mechanism of charmed particles. The cross section ranges indicated in fig.7 take into accaunt this model-dependence. The lower limits of our data correspond to the diffractive model and the upper limits to the $(1 - x)^N$ extrapolation.

Assuming a rise of charm cross sections with increasing energy, our results are in contradiction with the pp data from LEBC-EHS but they are compatible with the other pA data. The reason for these inconsistencies may be the A^{α} parametrization of charm cross sections, where α depends probably on x [23]. Moreover, an exact A^{α} parametrization predicts systematically too large cross sections on hydrogen for $\pi^{\pm}$, $K^{\pm}$ and $p/\bar{p}$ [24]. A similar behaviour for charm production can fake differences between results from pp and pA interactions.

Several attempts have been made to describe hadronic charm production by lowest-order QCD mechanisms [25-28]. For two such mechanisms the energy dependence of cross sections is illustrated in fig.7. The experimentally measured values appear to lie above the most theoretical predictions. The pA experiments and our data suggest a

Fig.7 Cross sections of $D/\bar{D}$ meson production ($x > 0$) in pp, pA and nC interactions. The curves are model calculations: (1) charm creation with $m_c = 1.3$ GeV/c^2 /25/, (2) charm excitation with $m_c = 1.3$ GeV/c^2 and $Q_0^2 = m_c^2/2$ /25/, (3) charm excitation with $m_c = 1.5$ GeV/c^2 and $Q_0^2 = m_c^2/2$ /26/.

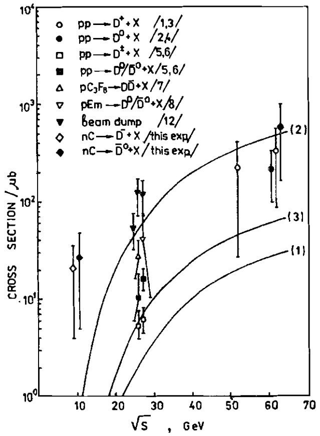

smoother rise of the cross section below $\sqrt{s} \sim 26$ GeV than expected so far from theoretical estimates. An explanation of this behaviour could be a different energy dependence of $\Lambda_c^+\bar{D}$ and $D\bar{D}$ production. At low energies charm should be produced mainly in $\Lambda_c^+\bar{D}$ final states, while $D\bar{D}$ production would become more important with increasing energy. Qualitatively, such a behaviour was observed for strange particle production in ΛK and $K\bar{K}$ final states /29/.

5. SUMMARY

The first measurement of inclusive $\bar{D}$ meson production in neutron-carbon interactions at 40 - 70 GeV/c has been reported. The $\bar{D}^0$ and D^- mesons were detected via the hadronic decay modes into $K^+(892)\pi^-$ and $K^+(892)\pi^-\pi^-$, respectively. In the kinematical region $x > 0.5$ and $p_T < 1$ GeV/c the following production properties can be summarized:

- The inclusive $\bar{D}$ cross sections are $\sigma_{\bar{D}^0} = (28 \pm 14)$ μb and $\sigma_{D^-} = (26 \pm 13)$ μb per carbon nucleus.
- The invariant longitudinal momentum spectra can be described in terms of $(1 - x)^N$ with $N_{\bar{D}^0} = 1.1 \pm 0.5 \pm 0.4$ and $N_{D^-} = 0.8 \pm 0.4 \pm 0.4$.
- The transverse momentum spectra are consistent with an exponential p_T^2 behaviour having slopes $B_{\bar{D}^0} = (1.2 {}^{+1.1}_{-0.9})$ $(\mathrm{GeV}/c)^{-2}$ and $B_{D^-} = (1.8 {}^{+1.3}_{-1.0})$ $(\mathrm{GeV}/c)^{-2}$.

Comparing with the Λ_c^+ production properties measured in the same experiment /13/, the following conclusions can be drawn:

- The $\bar{D}$ and Λ_c^+ production cross sections agree within the errors indicating the dominance of $\Lambda_c^+\bar{D}$ over $D\bar{D}$ production in the large x region. The nonobservation of the charge conjugated mesons D^0 and D^+ supports this hypothesis.
- The flat and similar longitudinal momentum spectra of Λ_c^+ and $\bar{D}$ points to $\Lambda_c^+\bar{D}$ production in diffraction-like processes.

Finally, the cross sections per nucleon for $x > 0$ were estimated assuming that the A dependence of $\bar{D}$ cross sections can be described by $A^{0.7}$ as measured for Λ_c^+ production in the same experiment /22/. The extrapolation to $x > 0$ was performed with i) a diffractive model and ii) a $(1 - x)^N$ parametrization. From this extrapolation we conclude:

- The model i) provides the lowest cross sections, ~ 10 μb per nucleon, whereas model ii) leads to large cross sections of 20 - 30 μb per nucleon.
- The comparison with data at higher energies /1-11/ suggest a smooth rise of charm cross sections below $\sqrt{s} \sim 26$ GeV.
- The charm cross section at $\sqrt{s} \sim 10$ GeV is larger than so far theoretically expected in the framework of perturbative QCD /25-28/.

The authors are grateful to A.M.Baldin, P.A.Cherenkov, Yu.N.Denisov, N.N.Govorun, Kh.Ya.Khristov, K.Lanius, A.A.Logunov, M.G.Meshcheryakov, I.A.Savin, A.N.Sissakian, L.D.Soloviev, A.N.Tavkhelidze, N.E.Tyurin, I.S.Zlatev, I.P.Kolpakov, and E.I.Maltsev for their support of these studies, to the staffs of the Serpukhov accelerator for their help in setting up and running this experiment.

REFERENCES

/1/ D.Drijard et al., Phys. Lett., 1979, 81B, p. 250.

/2/ G.Sajot, Proc. of the XXth Int. Conf. on High-Energy Physics, Madison 1980, p. 192.

/3/ M.Basile et al., Nuovo Cimento, 1982, 67A, p. 40.

/4/ M.Basile et al., Nuovo Cimento, 1981, 65A, p.457.

/5/ M.Aguilar-Benitez et al., Phys. Lett., 1984, 135B, p. 237.

/6/ M.C.Touboul, Proc. of the Int. Europhys. Conf. on High-Energy Physics, Bari 1985, p. 276.

/7/ S.Tavernier, Proc. of the XXIIth Int. Conf. on High-Energy Physics, Leipzig 1984, Vol.1 p. 161;
O.Erriquez et al., subm. to Physics Letters.

/8/ T.Aziz et al., Z.Phys.C-Particles and Fields, 1984, 26, p. 13.

/9/ H.Abramowicz et al., Z.Phys.C-Particles and Fields, 1982, 13, p. 179.

/10/ R.C.Ball et al., Phys. Rev. Lett., 1983, p. 743; R.J.Loveless, Proc. of the Int. Conf. Neutrino'82, Balatonfured 1982, p.89.

/11/ J.L.Ritchie et al., Phys. Lett., 1983, 126B, p. 499; A.Bodek et al., Rochester Univ. Report COO-3065-307, 1981.

/12/ T.Aziz, A.Gurtu, Z.Phys.C-Particles and Fields, 1983, 21, p.137.

/13/ A.N.Aleev et al., Yad. Fiz., 1982, 35, p. 1175; Ibid. 1983, 37, p. 1474; Ibid. 1986, 43, p. 619; A.N.Aleev et al., Z.Phys.C-Particles and Fields, 1984, 23, p.333.

/14/ A.N.Aleev et al., JINR E1-85-662, Dubna, 1985; Czech. J. Phys., 1986, B36, p.1303; subm. to Z.Phys.C - Particles and Fields.

/15/ G.Eichner et al., JINR 1-80-664, Dubna, 1980; JINR 13-80-161, Dubna, 1981; A.N.Aleev et al., JINR 1-81-67, Dubna, 1981; A.N.Maksimov et al., JINR 1-81-574, Dubna, 1981.

/16/ A.N.Aleev et al., JINR P1-82-353, Dubna, 1982; A.N.Aleev et al., PHE-82-7, Berlin-Zeuthen, 1982; A.N.Aleev et al., Yad. Fiz., 1986, 44, p. 661.

/17/ Particle data group, Phys. Lett., 1986, 170B, p.1.

/18/ V.V.Ammosov et al., Nucl. Phys., 1976, B115, p. 269; P.Skubic et al., Phys. Rev., 1978, D18, p. 3115.

/19/ S.J.Brodsky, J.F.Gunion, Phys. Rev., 1978, D17, p. 848; S.F.Gunion, Phys. Lett., 1979, 88B, p. 150; R.Blankenbecler, S.J.Brodsky, Phys. Rev., 1974, D10, p. 2973.

/20/ D.Cutts et al., Phys. Rev. Lett., 1978, 40, p. 141; Ibid., 1979, 43, p. 319; J.Singh et al., Nucl. Phys., 1978, B140, p. 189; A.K.Nandi et al., Nucl. Phys., 1980, B169, p. 20.

/21/ T.Bowcock et al., Phys. Rev. Lett., 1985, 55, p. 923.

/22/ H.Nowak, Proc. of the XXIIth Int. Conf. on High-Energy Physics, Leipzig 1984, Vol.1 p. 158; A.N.Aleev et al., subm. to the XXIIIth Int. Conf. on High-Energy Physics, Berkeley 1986; A.N.Aleev et al., JINR D1-86-442, Dubna, 1986.

/23/ D.S.Barton et al., Phys. Rev., 1983, D27, p. 2580.

/24/ M.G.Abreu et al., Z.Phys.C-Particles and Fields, 1984, 25, p.115; A.E.Brenner et al., FERMILAB-Conf-80/47-EXP, Batavia, 1980.

/25/ B.L.Combridge, Nucl. Phys., 1979, B151, p. 429.

/26/ R.Odorico, Nucl. Phys., 1982, B209, p. 77; R.Odorico, Proc. of the Moriond Workshop on New Flavours, Les Arcs 1982.

/27/ R.Winder, C.Michael, Nucl.Phys., 1980, B173, p. 59.

/28/ S.N.Ganguli, M.Schouten, Z.Phys.C-Particles and Fields, 1983, 19, p. 83.

/29/ R.Gottgens et al., Z.Phys.C-Particles and Fields, 1983, 19, p. 283; H.Fesefeldt et al., Nucl. Phys., 1979, B147, p. 317.

Received by Publishing Department
on April 17, 1987.

Алеев А.Н. и др. E1-87-265

Рождение $\bar{D}^{o}$- и D^{-}-мезонов в нейтрон-углеродных взаимодействиях при 40-70 ГэВ

Исследовалось образование $\bar{D}$-мезонов в нейтрон-углеродных взаимодействиях при 40-70 ГэВ/с. $\bar{D}$-мезоны наблюдены по адронным модам распада $D^{o} \to K^{+}(892)\pi^{-}$ и $D^{-} \to K^{+}(892)\pi^{-}\pi^{-}$. В кинематической области $x > 0,5$ и $p_T < 1$ ГэВ/с получены величины инклюзивных сечений на ядро углерода $\sigma_{\bar{D}^{o}} = (28 \pm 14)$ мкб и $\sigma_{D^-} = (26 \pm 13)$ мкб. Инвариантные спектры продольных импульсов могут быть представлены в виде $(1-x)^N$ с $N_{\bar{D}^{o}} = 1,1 \pm 0,5 \pm 0,4$ и $N_{D^-} = 0,8 \pm 0,4 \pm 0,4$. Для спектров поперечных импульсов параметризованных в виде $\exp(-B \cdot p_T^2)$ получено: $B_{\bar{D}^{o}} = (1,2^{+1,1}_{-0,9})$ (ГэВ/с)$^{-2}$ и $B_{D^-} = (1,8^{+1,3}_{-1,0})$ (ГэВ/с)$^{-2}$.

Работа выполнена в Лаборатории высоких энергий ОИЯИ.

Препринт Объединенного института ядерных исследований. Дубна 1987

Aleev A.N. et al. E1-87-265

Production of $\bar{D}^{o}$ and D^{-} Mesons in Neutron in Neutron-Carbon Interactions at 40-70 GeV

The production of $\bar{D}$ mesons in neutron-carbon interactions at 40-70 GeV/c has been investigated. The $\bar{D}$ mesons were detected via the hadronic decay modes $\bar{D}^{o} \to K^{+}(892)\pi^{-}$ and $D^{-} \to K^{+}(892)\pi^{-}\pi^{-}$. In the kinematic region $x > 0.5$ and $p_T < 1$ GeV/c the following inclusive cross sections were measured: $\sigma_{\bar{D}^{o}} = (28 \pm 14)$ μb and $\sigma_{D^-} = (26 \pm 13)$ μb per carbon nucleus. The invariant longitudinal momentum spectra can be described by $(1-x)^N$ with $N_{\bar{D}^{o}} = 1.1 \pm 0.5 \pm 0.4$ and $N_{D^-} = 0.8 \pm 0.4 \pm 0.4$. The transverse momentum spectra were parametrized by $\exp(-B \cdot p_T^2)$ with $B_{\bar{D}^{o}} = (1.2^{+1.1}_{-0.9})$ (GeV/c)$^{-2}$ and $B_{D^-} = (1.8^{+1.3}_{-1.0})$ (GeV/c)$^{-2}$.

The investigation has been performed at the Laboratory of High Energies, JINR.

Preprint of the Joint Institute for Nuclear Research. Dubna 1987